MRS Communications

https://doi.org/10.1557/s43579-025-00842-6

MRS Communications

Research Letter

Extracting thermoelectric parameters from hierarchically designed thinner Peltier sheets

Norifusa Satoh, and Jin Kawakita, National Institute for Materials Science (NIMS), Tsukuba 305-0044, Japan
Junnosuke Murakami, and Junichi Nakadate, Sekisui Chemical Company, Limited, Osaka 618-0021, Japan
Address all correspondence to Norifusa Satoh at **SATOH.Norifusa@nims.go.jp**

(Received 21 July 2025; accepted 16 September 2025)

Abstract

To respond to the growing extreme heatwaves, we have adapted a multi-component strategy on thermoelectrics (TEs) to enlarge the cooling area and slim the weight of Peltier devices. We design the sticky TE complexes to be deformable and encapsulated within electrodes and foam sheets, facilitating a roll-to-roll production process. However, due to their deformability, we are unable to obtain their TE parameters based on the analytic tradition in TEs. To address this limitation, we adapted a methodology from coordination chemistry dealing with complexities to extract TE parameters from a series of thinner Peltier sheets, paving the way for future improvements.

Introduction

Record-breaking extreme heat events threaten people's survival, health, and wellbeing.[1] Since the 25–50% of humankind faces deadly heatwave without indoor cooling,[2] the United Nations launched the Global Cooling Pledge to deriver highly efficient air conditioners worldwide.[3] Still, there is a technological gap between the current cooling capability and the future demand toward net zero emission by 2050.[4] Peltier human cooling devices can be nominated as a potential filler, because the direct cooling of human body suppresses the start and power of air conditioners, saving energy consumption 10-times more than air conditioners only.[5] Yet, their heaviness, solidness, and limited cooling area disadvantage the global distribution of Peltier human cooling devices.

To respond to the growing extreme heatwaves threatening human lives, we have adapted a multi-component strategy on thermoelectrics (TEs) to enlarge the cooling area and slim the weight of Peltier devices.[4,6–10] To achieve this, we design the sticky TE complexes as a deformable substance to be encapsulated within electrodes and foam sheets in a three-step process [Fig. 1(a)] with a prospect to mass-produce thinner Peltier sheets *via* a roll-to-roll process without using electrically conductive adhesives.[6] The hierarchical design turns element composition of TE particles for high Seebeck coefficient, α, at atomic scale,[8] controls the surface of TE particles for small electrical resistivity, ρ, at nano scale[8], minimizes thermal conductivity, κ, and absorbs mechanical bending stress by hybridizing organic solvent with the TE particles[7] and adopts ultra-thin high performance foam sheets at micro scale,[10] and patterns the sticky TE complexes and electrodes to reduce Joule heating loss at macro-scale[4] [Fig. 1(b)]. Since Peltier sheets enhance the heat flux capability as thinner [Fig. 1(c)],[9,10] the cooling potential overcomes the metabolic rate of human body.[4]

Due to the deformability of the sticky TE complexes, however, conventional analytic methods are not suitable for measuring their TE parameters. From a solid-state physics perspective, the analytic tradition is designed well to evaluate solid TE materials based on the definition of materials properties. In a four-probe measurement condition applying a current, I, or a temperature gradient, ΔT, on TE materials from the outer probes, the inter probes can detect a voltage drop, IR, caused by I to calculate the ρ and a thermovoltage, V, caused by the temperature gradient between the probes, $\Delta T'$, to obtain the α [Fig. 2(a)]. Under a condition monitoring the surface temperature of TE materials T, a laser flash from the other side generates heat for thermal diffusion to determine the κ [Fig. 2(b)]. Note that reliable TE parameter analyses require the certain volume of sample to define the accurate dimensions; for example, as standardized by JIS R 1650–1, -2, and -3.

Since we need to specify the dimensions of sticky TE complexes, in our previous study, we have tentatively calculated the ρ from the resistance R and the dimensions and the α from the V and the ΔT measured from the outside, using a single cell structure capsulating the deformable sticky TE complexes.[8] These tentative calculations overestimate the ρ because the R includes the interfacial resistance with the electrodes and underestimate the α due to the temperature drop on the electrode sheets, $\Delta T - \Delta T'$. Furthermore, the effective κ is composed of those of TE particles, organic solvent, and foam sheets.[7,10] Overall, while the physical properties of solid TE materials have been accurately evaluated and then assembled into the devices, it remains an open question how to evaluate whether the individual TE parameters of components behave as expected under a working condition after the device fabrication processes.

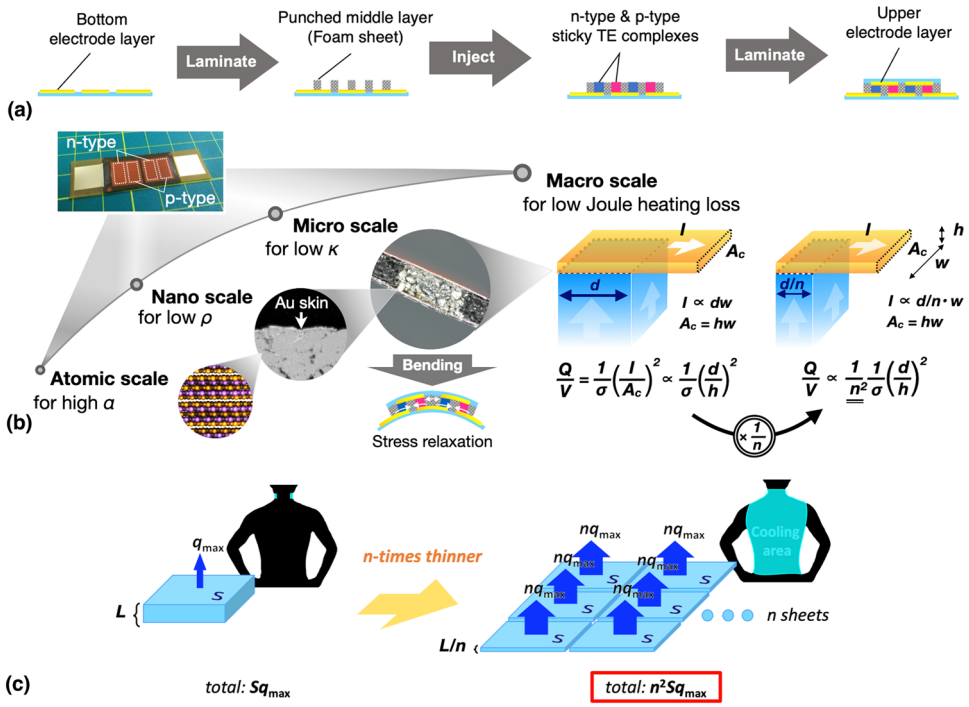

Figure 1. Progress summary of thinner Peltier sheets using the sticky TE complexes.[4,6–10] (a) Schematic cross-section for the three-step fabrication of the hierarchically designed thinner Peltier sheets using the sticky TE complexes. (b) Hierarchical design of thinner Peltier sheets at atomic-, nano-, micro-, and macro-scale, where Q is Joule heating per unit time, V is volume, σ is electrical conductivity of electrode, I is current, A_c is cross-sectional area of electrode, h is height of electrode, w is width of electrode and sticky TE complexes' pattern, and d is depth of sticky TE complexes' pattern. (c) Schematic comparison in the total Sq_{max} between a L-thick Peltier device and n sheets of L/n-thick Peltier sheets, using the same amount of TE material, where S is surface area, L is thickness, and q_{max} is the maximum heat flux capability.

When confronted with a complexity of multi-component complexes, we can adapt the conceptual framework and methodology from coordination chemistry for metal complexes known by Nobel prize in Chemistry 1913.[11] Coordination chemistry deals with "metal complexes" where metal ions coordinate with ligands through multiple interactions in solution. To determine the binding constants between metal ions and ligands, complexometric titration is a common method gradually changing only the concentration of titrants during monitoring the changes of analytes.[12,13] During the titration for a single coordination process, isosbestic points appear in the spectral change when the spectra for the initial and final states have cross points.[11] Consequently, the shift of isosbestic points distinguishes multistep processes in multiple interactions.[12] The concept has been generalized to explain iso-points[11] observed in Raman spectra,[14] photoluminescence,[15] cyclic voltammetry,[11,16] specific heat curves of correlated systems,[17] optical absorption in atomic-layer superlattices,[18] magnetics of perovskite oxides,[19] and current–voltage curves in photovoltaics.[11,20] In essence, gradually and continuously altering one parameter is a straightforward and powerful method to comprehend one aspect of complexity step-by-step.

Although one of the TE parameters itself is not defined by the dimensions: $\alpha = V/\Delta T'$, we set a working hypothesis to extract the TE parameters from a series of thinner Peltier sheets only changing the L under a constant ΔT condition [Fig. 2(c, d)], inspired by the insight generalized from coordination chemistry. To change the L, we can stack the middle layers [Fig. 2(e)]. Under the temperature gradient of ΔT, a battery tester[9] can measure the V and the R at each L, using an alternating-current (AC) signal [Fig. 2(c)]. Note that a tester using a direct current (DC) cannot correctly evaluate the R assuming Ohm's law because the V caused by ΔT affects the IR. Following the definition: $R = \rho L/A$, we can extract the ρ in the plot of L/A versus R, where A is the total contact area. To extract the α, we assume a linear temperature gradient on the Peltier sheets so that we can describe the temperature difference on the sticky TE complexes $\Delta T' = \Delta T \cdot (L - 2t)/L$ [Fig. 2(e)], where t is thickness of electrode sheet. Under this assumption, $V = \alpha \Delta T' = \alpha \Delta T \cdot (1 - 2t/L)$. Thus, we can obtain the α from the intercept $\alpha \Delta T$ in the plot of $1/L$ versus V. As a result, we can calculate $\Delta T'$ from V on each L, as follows: $\Delta T' = V/\alpha$. Therefore, we can also extract the effective κ based on the definition: $q/\Delta T' = \kappa/(L - 2t)$ where a heat flux sensor quantifies the heat flux q on each L [Fig. 2(d)]. In summary, the working hypothesis is examined using the coefficient of determination, R^2, for the simple linear regressions [Fig. 2(c, d)]. However, a commercially available heat flux sensor only covers half of

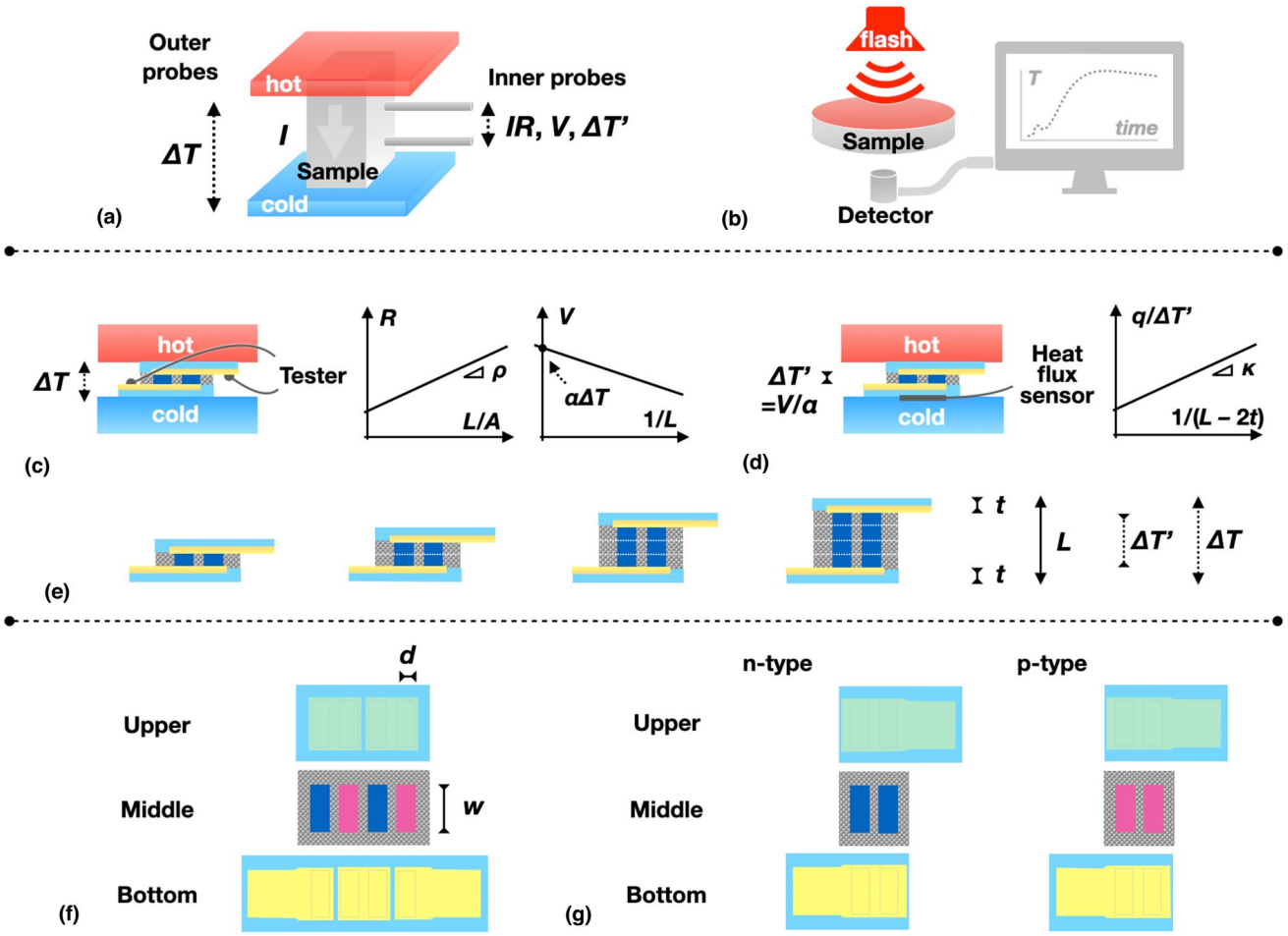

Figure 2. Analytic tradition to evaluate TE materials: (a) Four-probe measurement for ρ and α under a temperature gradient condition, (b) Laser flash method for κ. Schematic cross-section for TE parameter extraction from a series of Peltier sheets changing *L* under a constant *ΔT* condition: (c) ρ and α extraction, (d) κ extraction, (e) Peltier sheets changing *L* based on the number of stacking middle layers. (f) Top view of each layer for the current Peltier sheet with a stripe pattern in series, where the cell area *dw* is 4 mm × 10 mm and the line space is 2 mm. (g) Top view of each layer for half Peltier sheets with the stripe pattern in parallel to extract the TE parameters.

the current Peltier sheet patterning, which consists of n-type/p-type/n-type/p-type stripes in series [Fig. 2(f)].[4] In this study, therefore, we prepare half Peltier sheets of $A = 2dw$ patterning n-type/n-type and p-type/p-type stripes in parallel to examine the working hypothesis and extract the TE parameters of n-type and p-type sticky TE complexes, respectively [Fig. 2(g)]. Since we obtain reasonable TE parameters of sticky TE complexes with $R^2 > 0.9$, we further discuss the potential improvements in the thinner Peltier sheets based on the obtained results.

Experimental details

The half Peltier sheets were assembled by the previous method[4,6–10] with the following modifications: The sticky TE complexes of partial Au skin Bi_2Te_3 particles were prepared as previously described.[8] The upper and bottom electrode sheets were fabricated as single-side flexible printed circuits (FPCs) by Scott Design System Co., Ltd., Japan. As the punched middle layer, the ultra-thin high performance foam (thickness: 0.3 mm, XLIM, Sekisui Chemical Co., Ltd., Japan) with double-coated adhesive was laminated to alter the *L* and subsequently cut according to a programed pattern using a laser-cutting machine (VLS2.30DT, Universal Laser Systems, USA). After the underside of middle layers was sealed with the bottom electrode sheets, the hierarchically designed sticky TE complexes were injected into the patterned areas. The injection amount of sticky TE complexes was determined based on the capsule volume, calculated from the thickness of middle layers and two adhesive layers and the area of cut patterns. Finally, the deformable sticky TE complexes were sealed with the upper electrode sheets [Fig. 1(a)]. The *L* and *t* were measured with a digital micrometer (MDC-25MX, Mitutoyo Corporation, Japan). To measure *R* and *V* at each *L* with a battery tester (BT3562A, Hioki E.E. Corporation, Japan), the bottom side of half Peltier sheets was cooled with an air-cooling Peltier plate (CHP-77HI, Sensor Controls Co., Ltd., Japan) set at 20ºC, and

the upper side was heated by a hot plate (PH200-100-PCC10A, MSA Factory Co., Ltd., Japan) set at 40ºC. The interfaces were filled with a thermal grease (SMZ-01R, Shinwa Sangyo LTD., Japan). The applied ΔT and q were measured with a thermocouple (ST-11 K-008-TS1-ASP, Anritsu Meter Co., Ltd., Japan) and a heat flux sensor equipped with a thermocouple (Z2012-01, DENSO Corporation, Japan). These measurements were monitored with a data logger (LR8432, Hioki E.E. Corporation, Japan). Note that the battery tester provides the equivalent data of R and V for those estimated from the I-V characteristics written in the previous paper.[8,9]

Results and discussion

Figure 3 displays the graphs to extract the TE parameters of sticky TE complexes from a series of thinner Peltier sheets only changing the thickness L based on the number of stacking middle layers, 1 to 4. As defined, the L increased the R due to the lengthened conduction pathway. The slope in graphs of L/A versus R corresponds to the ρ to be 179 μΩm and 180 μΩm for the p-type and n-type sticky TE complexes, respectively [Fig. 3(a),(b)]. The V also increased with the L because the $\Delta T - \Delta T'$ ultimately becomes ignorable at the infinite L. Because of this, the intercept in graphs of $1/L$ versus V represents the $\alpha\Delta T$, which allow to extract the α to be 138 μV/K and –87.4 μV/K for the p-type and n-type sticky TE complexes, respectively [Fig. 3(c,d)]. Based on the extracted α with the measured V on each L, we can access the $\Delta T'$. Thus, we can plot the graphs of $q/\Delta T'$ versus $1/(L - 2t)$ to extract the κ: 0.10 W/mK and 0.12 W/mK for the p-type and n-type sticky TE complexes, respectively [Fig. 3(e, f)]. Since all the plots are linearly fitted with $R^2 > 0.9$, these results fairly support the working hypothesis to extract the TE parameters.

These extracted values appear reasonable in comparison with those of the tentative analysis and the original TE particles (Table I). Since the interfacial electrical resistances with the electrodes were successfully subtracted, the extracted ρ became approximately 10-times smaller than that of the tentative analyzed ones. Nevertheless, the extracted ρ is approximately 20-times higher than that of the original TE materials before crushing because the interfacial electrical resistances persist between the TE particles even after the surface of TE particles is partially covered with low-resistance Au.[8] Similarly, the extracted α became comparable to that of the original TE materials because the $\Delta T - \Delta T'$ approaches zero at the extrapolated intercepts. The extracted κ lessened 10 times than that of the original TE materials, which is consistent with the previous observations.[7,10] As visualized with a thermal imager,

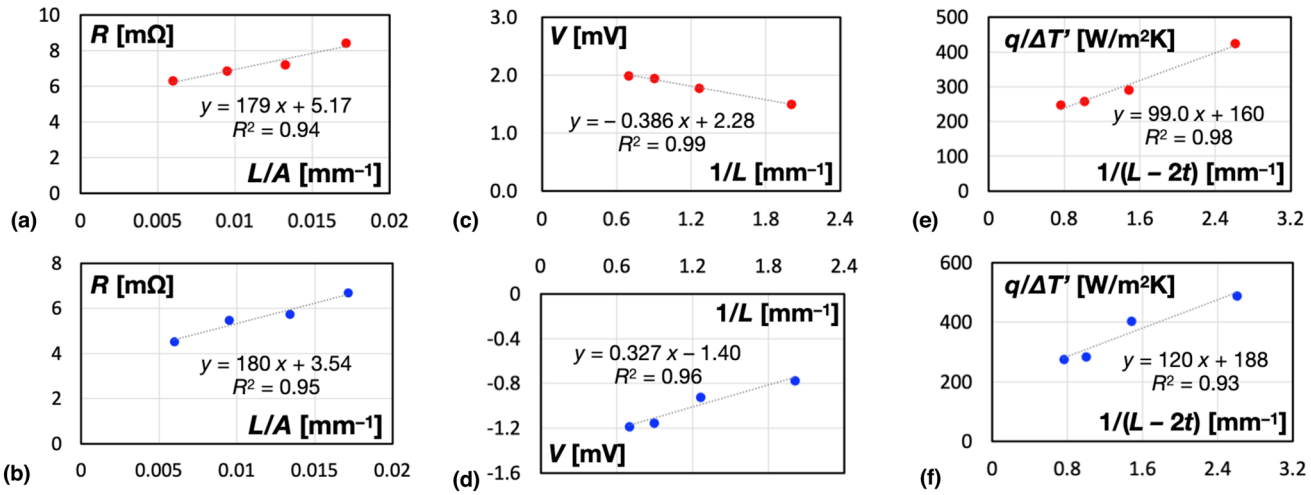

Figure 3. Graphs of L/A versus R to extract the ρ of (a) p-type and (b) n-type sticky TE complexes, $1/L$ versus V to extract the α of (c) p-type and (d) n-type sticky TE complexes, and $1/(L - 2t)$ versus $q/\Delta T'$ to extract the κ of (e) p-type and (f) n-type sticky TE complexes.

Table I. Summary and comparison of the extracted TE parameters.

	p-type				n-type			
	ρ (μΩm)	α (μV/K)	κ (W/mK)	zT	ρ (μΩm)	α (μV/K)	κ (W/mK)	zT
This work	179	138	0.10	0.32	180	–87.4	0.12	0.11
Tentative[8]	$1.7 \cdot 10^3$	95.3	–	–	$1.2 \cdot 10^3$	–75.9	–	–
Original	10.9	183	1.0	0.96	7.4	–149	1.0	0.94
Best reports[22,23]	15.4	242	0.65	1.86	12.1	–234	0.80	2.27

the κ surrounded with the polymer middle layer drastically has decreased close to that of organics, ~0.2 W/mK, explained by the Kanari equation.[7] Replacing the middle layer with the foam sheet, the performance of Peltier sheets has almost doubled.[10] This implies that the surrounding foam sheet has halved the κ, which is in agreement with the extracted κ. In total, the current $zT = \alpha^2/\rho\kappa \cdot T$ can be calculated to be 0.32 and 0.11 for the p-type and n-type sticky TE complexes, respectively.

Extracting the TE parameters from the thinner Peltier sheets indicates opportunities for enhancing their performance. Firstly, this research demonstrated that the R is attributed to the interfacial electrical resistances between the sticky TE complexes and the electrodes. As previously discussed, Joule heating on electrodes diminishes the cooling capacity based on the Peltier effect.[4] Similarly, the confirmed interfacial electrical resistances for Joule heating prejudice the cooling capacity. Conversely, reducing the interfacial electrical resistances could enhance the practical performances of thinner Peltier sheets. To reduce the interfacial electrical resistances, we can possibly deposit low temperature solders[21] like Sn–Bi, Sn–In, or Sn–Bi–In on electrodes, considering the heat-resistant temperature of foam. Secondly, the original TE materials exhibit higher α and lower ρ than the thinner Peltier sheets because of the difference in synthetic process. Generally, inorganic TE materials are synthesized by sintering at high pressure and high temperature to improve the crystallinity and electrical conduction path.[22,23] This suggests that the thinner Peltier sheets may improve their performances by additives linking the TE particles and post treatments. Lastly, the current TE particles still have a margin to improve α in comparison with the best reports in Bi–Te-based TE materials.[22,23] Overall, this research leads to reject the statement "without using electrically conductive adhesives"[6] in the initial working hypothesis of sticky TE complexes and reconstruct the multi-component design and fabrication process of the thinner Peltier sheets toward the next phase.

Conclusion

By adapting a methodology from coordination chemistry to address the complex system of thinner Peltier sheets, we have successfully extracted the TE parameters with $R^2 > 0.9$ from a series of half Peltier sheets only changing the L under a constant ΔT condition. This approach is potentially applicable to other TE devices by comparing the extracted TE parameters with those of original TE materials. Having established the analytic method, we can sophisticate the multi-component strategy of thinner Peltier sheets through the cycle of design and analysis toward the higher order complex system. At the end of this research cycle, the new class of materials may safeguard people from frequent and intense extreme heat events.

Acknowledgments

The authors would like to thank Misaki Itakura for her technical assistance.

Author contributions

Norifusa Satoh designed the study concept, defined the experimental condition, and analyzed the data to write the first draft of the manuscript based on the discussion with all authors. Junnosuke Murakami selected the appropriate foam sheet for this study and provided the handing instruction. All authors commented on the first draft to approve the manuscript.

Funding

This study was supported by New Energy and Industrial Technology Development Organization (NEDO), JPNP20004, Norifusa SATOH.

Data availability

The data generated during the current study are available from the corresponding author on reasonable request.

Declarations

Conflict of Interest

On behalf of all authors, the corresponding author states that there is no conflict of interest.

References

1. M. Romanello, M. Walawender, S.-C. Hsu, A. Moskeland, Y. Palmeiro-Silva, D. Scamman et al., The 2024 report of the Lancet countdown on health and climate change: facing record-breaking threats from delayed action.

Lancet **404**(10465), 1847–1896 (2024). https://doi.org/10.1016/S0140-6736(24)01822-1
2. International Energy Agency. Sustainable, Affordable Cooling Can Save Tens of Thousands of Lives Each Year. (March 2023), https://www.iea.org/reports/sustainable-affordable-cooling-can-save-tens-of-thousands-of-lives-each-year Accessed 16 July 2025
3. United Nations Environment Programme. Global Cooling Pledge for COP28. (December 2023), https://wedocs.unep.org/bitstream/handle/20.500.11822/44310/Global-Cooling-Pledge-final_231206_145613.pdf Accessed 16 July 2025
4. N. Satoh, J. Kawakita, J. Murakami, Macro-scale patterning for hierarchically designed thinner Peltier sheets. MRS Adv. **9**(21), 1643–1648 (2024). https://doi.org/10.1557/s43580-024-00937-7
5. K. Itao, H. Hosaka, K. Kiiaka, M. Takahashi, G. Lopes, Wearable equipment development for individually adaptive temperature-conditioning. J. Jpn. Soc. Precis. Eng. **82**, 919–924 (2016). https://doi.org/10.2493/jjspe.82.919
6. N. Satoh, M. Otsuka, T. Ohki, A. Ohi, Y. Sakurai, Y. Yamashita, T. Mori, Organic π-type thermoelectric module supported by photolithographic mold: a working hypothesis of sticky thermoelectric materials. Sci. Technol. Adv. Mater. **19**(1), 517–525 (2018). https://doi.org/10.1080/14686996.2018.1487239
7. N. Satoh, M. Otsuka, Y. Sakurai, T. Asami, Y. Goto, T. Kawamori, T. Masaki, G. Yatabe, J. Kawakita, T. Mori, Sticky thermoelectric materials for flexible thermoelectric modules to capture low-temperature waste heat. MRS Adv. **5**(10), 481–487 (2020). https://doi.org/10.1557/adv.2020.84
8. N. Satoh, M. Otsuka, J. Kawakita, T. Mori, A hierarchical design for thermoelectric hybrid materials: Bi_2Te_3 particles covered by partial Au skins enhance thermoelectric performance in sticky thermoelectric materials. Soft Sci. **2**(3), 15 (2022). https://doi.org/10.20517/ss.2022.15
9. N. Satoh, M. Otsuka, J. Kawakita, Hierarchically designed sticky thermoelectric materials to fabricate thinner Peltier sheets and device architectures. MRS Adv. **8**(8), 446–450 (2023). https://doi.org/10.1557/s43580-023-00541-1
10. N. Satoh, J. Kawakita, J. Murakami, J. Nakadate, T. Nakanishi, Sticky thermoelectric materials collaborate with ultra-thin high performance foam for hierarchically designed flexible peltier sheets. MRS Adv. **8**(15), 781–786 (2023). https://doi.org/10.1557/s43580-023-00631-0
11. N. Satoh, L. Han, Chemical input and *I-V* output: stepwise chemical information processing in dye-sensitized solar cells. Phys. Chem. Chem. Phys. **14**(46), 16014–16022 (2012). https://doi.org/10.1039/C2CP43460A
12. N. Satoh, T. Nakashima, K. Kamikura, K. Yamamoto, Quantum size effect in TiO_2 nanoparticles prepared by finely controlled metal assembly on dendrimer templates. Nat. Nanotechnol. **3**(2), 106–111 (2008). https://doi.org/10.1038/nnano.2008.2
13. N. Satoh, T. Watanabe, Y. Iketaki, T. Omatsu, M. Fujii, K. Yamamoto, Formation of nano-dots of phenylazomethine dendrimers with Rhodamine 6G on mica. Polym. Adv. Technol. **15**(4), 159–163 (2004). https://doi.org/10.1002/pat.378
14. D.N. Whiteman, G.E. Walrafen, W.-H. Yang, S.H. Melfi, Measurement of an isosbestic point in the Raman spectrum of liquid water by use of a backscattering geometry. Appl. Opt. **38**(12), 2614–2615 (1999). https://doi.org/10.1364/AO.38.002614
15. I.L. Medintz, A.R. Clapp, H. Mattoussi, E.R. Goldman, B. Fisher, J.M. Mauro, Self-assembled nanoscale biosensors based on quantum dot FRET donors. Nat. Mater. **2**(8), 630–638 (2003). https://doi.org/10.1038/nmat961
16. H.J. Paul, J. Leddy, Direct determination of the transfer coefficient from cyclic voltammetry: isopoints as diagnostics. Anal. Chem. **67**(10), 1661–1668 (1995). https://doi.org/10.1021/ac00106a003
17. D. Vollhardt, Characteristic crossing points in specific heat curves of correlated systems. Phys. Rev. Lett. **78**(7), 1307–1310 (1997). https://doi.org/10.1103/PhysRevLett.78.1307
18. X. Zhai, C.S. Mohapatra, A.B. Shah, J.-M. Zuo, J.N. Eckstein, New optical absorption bands in atomic-layer superlattices. Adv. Mater. **22**(10), 1136–1139 (2010). https://doi.org/10.1002/adma.200904197
19. A.A. Belik, Y. Matsushita, M. Tanaka, E. Takayama-Muromachi, $(In_{1-y}Mn_y)MnO_3$ ($1/9 \le y \le 1/3$): unusual perovskites with unusual properties. Angew. Chem. Int. Ed. **49**(42), 7723–7727 (2010). https://doi.org/10.1002/anie.201003080
20. Y. Dong, B. Tian, T.J. Kempa, C.M. Lieber, Coaxial group III–nitride nanowire photovoltaics. Nano Lett. **9**(5), 2183–2187 (2009). https://doi.org/10.1021/nl900858v
21. Y. Liu, K.N. Tu, Low melting point solders based on Sn, Bi, and In elements. Mater. Today Adv. **8**, 100115 (2020). https://doi.org/10.1016/j.mtadv.2020.100115
22. S.I. Kim, K.H. Lee, H.A. Mun, H.S. Kim, S.W. Hwang, J.W. Roh, D.J. Yang, W.H. Shin, X.S. Li, Y.H. Lee, G.J. Snyder, S.W. Kim, Dense dislocation arrays embedded in grain boundaries for high-performance bulk thermoelectrics. Science **348**(6230), 109–114 (2015). https://doi.org/10.1126/science.aaa4166
23. H. Choi, K. Jeong, J. Chae, H. Park, J. Baeck, T.H. Kim, J.Y. Song, J. Park, K.-H. Jeong, M.-H. Cho, Enhancement in thermoelectric properties of Te-embedded Bi_2Te_3 by preferential phonon scattering in heterostructure interface. Nano Energy **47**, 374–384 (2018). https://doi.org/10.1016/j.nanoen.2018.03.009